Journal of Neuroradiology 46 (2019) 384–389

Available online at ScienceDirect www.sciencedirect.com

Elsevier Masson France EM|consulte www.em-consulte.com

Original Article

Efficacy of post-dilatation during carotid artery stenting for unstable plaque using closed-cell design stent evaluated by optical coherence tomography

Kei Harada*, Masahito Kajihara , Yukihiro Sankoda , Syunsuke Taniguchi

Department of Neurosurgery, Fukuoka Wajiro Hospital, 2-2-75, Wajirogaoka, Higashi-Ku, Fukuoka-city, 811-0213 Fukuoka, Japan

ARTICLE INFO

Article history:
Available online 4 April 2019

Keywords:
Carotid artery stenting
Optical coherence tomography
Post-dilatation
In-stent tissue prolapse

ABSTRACT

Background and purpose. – This study aimed to use optical coherence tomography (OCT) to evaluate the efficacy of post-dilatation (PD) after stent placement for unstable plaques during carotid artery stenting (CAS) using closed-cell design stent.

Materials and methods. – Twelve unstable carotid plaque lesions diagnosed by magnetic resonance imaging were evaluated by OCT during CAS. Pre-procedural minimum lumen diameter and area were 1.5 ± 0.6 mm and 2.6 ± 1.6 mm^2, respectively. The lesion was pre-dilated with balloon catheters (diameter 4.8 ± 0.3 mm), and closed-cell stent was deployed. PD was performed with balloon catheters of the same size as those used for pre-dilatation. Minimum lumen diameter/area and in-stent tissue prolapse volume after stent placement and after PD were calculated by 2-dimensional cross section images. The number of the stent cells showing tissue prolapse and malapposition after stent-placement and after PD were calculated by 3-dimensional analysis.

Results. – Compared to after stent placement, in-stent tissue prolapse volume (0.18 ± 0.10 to 0.22 ± 0.07 mm^2/slice, $P < 0.01$), number of stent cells with any tissue prolapse (12.7 ± 8.2 to 21.0 ± 11.8%, $P < 0.001$) were significantly increased after PD; stent cells with ≥ 500-μm tissue prolapse (1.6 ± 1.1 to 0.7 ± 0.8%, $P < 0.01$) and stent malapposition (17.4 ± 7.2 to 14.0 ± 6.3%, $P < 0.01$) were significantly decreased.

Conclusions. – PD after carotid stent placement caused increase in in-stent tissue prolapse volume and small tissue prolapse, however, the in-stent large tissue prolapse decreased, as the in-stent tissue prolapse may have been crushed into debris.

Introduction

Atherosclerotic carotid artery stenosis is the main cause of cerebral stroke. Carotid artery stenting (CAS) has emerged as a therapeutic alternative to carotid endarterectomy (CEA) for the treatment of carotid artery stenosis; however, the rate of ischemic complications with CAS is higher than that with CEA [1]. CAS for unstable plaques is associated with a high risk of ischemic complications [2], therefore, embolic protective devices (EPD) such as a distal filter or a proximal protection system have been developed to prevent intra-procedural ischemic events, and stents with a closed cell (CC) design have been used. CC stents have low adaptability to vessels and low cell size areas, and thus, there is lesser likelihood of plaque protrusion, hence, they have been frequently used for unstable carotid plaques [3]. However, the problems of plaque protrusion during CAS for unstable plaques still unsolved [4–6].

The CAS procedure generally involves lesion crossing, lesion pre-dilatation, stent placement, and post-dilatation (PD) with EPD. It has been observed that the PD procedure helped increase the in-stent lumen area; however, it increased procedure-related embolization because of fractured debris from the carotid plaque [7,8]. Although CAS with under-sized stent dilatation was safe during the procedure, the problems of delayed stent thrombosis due to insufficient stent dilatation and long-term restenosis remained [9]. Conventional evaluation methods such as intra vascular ultrasound and angiography, have not been useful in determining whether PD is related to in-stent tissue prolapse [10].

Therefore, the aim of this study was to use optical coherence tomography (OCT) during CAS using CC stents for unstable plaques

* Corresponding author at: Department of Neurosurgery, Fukuoka Wajiro Hospital, 2-2-75, Wajirogaoka, Higashi-Ku, Fukuoka-city, 811-0213 Fukuoka, Japan.
E-mail address: keihara@f-wajirohp.jp (K. Harada).

https://doi.org/10.1016/j.neurad.2019.03.006
0150-9861/

to detect stent dilatation, in-stent tissue prolapse, and stent malapposition, and to evaluated the efficacy of PD.

Materials and methods

From July 2016 to December 2017, carotid revascularization was performed for 110 lesions in 105 patients at our hospital. CEA and CAS were performed for 21 and 89 lesions, respectively. CEA was mainly performed for cases with unstable plaques and severe calcification without systemic complications. CAS was mainly performed for cases with stable plaques, and cases with a high risk of CEA, even if unstable plaques were present. In symptomatic cases, CAS was performed at least 2 weeks after symptoms. Written informed consent was obtained from all patients. Inclusion criteria were > 80% asymptomatic internal carotid artery (ICA) stenosis and > 50% symptomatic ICA stenosis. Plaques were diagnosed by MRI and ultrasound. OCT study during CAS was performed for 22 lesions defined as "unstable" on MRI. We did not include patients with creatinine levels > 1.2 mg/dL, and lesions with distal ICA elongation. In 12 of 22 lesions which PD was performed with same-size balloon catheter with pre-dilatation, OCT analysis was performed before pre-dilatation, after stent placement, and after PD. This study was retrospectively researched in the 12 lesions. Carotid ultrasound or contrast enhanced computed tomography was performed to examine restenosis and in-stent thrombosis during the follow-up period of at least 6 months.

Plaque MRI

Carotid MRI using a 3 T imaging machine (Magnetom Verio; Simens, Erlangen, Germany) was performed before the procedure. T1 and T2 weighted images of the carotid artery, including the area with the highest rate of stenosis and plaque, were obtained. T1 weighted image parameters were as follows: repetition time (TR), 500; echo time (TE), 13; and slice thickness, 2.0. T2 weighted image parameters were: TR, 4200; TE, 86; and slice thickness, 3.0 mm. The relative signal intensity (rSI) of plaque components was calculated in relation to the sternocleidomastoid muscle on T1 weighted images and in relation to the submandibular gland on T2 weighted images. On T1 weighted images, rSI > 1.5 was defined as "high", meaning unstable. On T2 weighted images, rSI > 1.5 was defined as "high".

CAS procedure

Local anesthesia was performed for all patients to allow continuous monitoring of the level of consciousness and motor function. Systemic anticoagulation was achieved by administration of heparin to maintain an activated clotting time of at least 275 sec. For 10 lesions, an 8 F or 9 F guiding catheter with a temporary occlusion balloon (Optimo; Tokai Medical Products) was navigated to the common carotid artery (CCA) from the femoral artery, a PurcuSurge Guardwire (Medtronic, Minneapolis, Minnesota, USA) was navigated to the external carotid artery (ECA), and a distal filter protection device (FilterWire EZ; Stryker, Fremont, California, USA, or Spider FX; Medtronic, Minneapolis, Minnesota, USA) crossed the stenotic lesions with CCA and ECA occlusion. Distal protection was achieved using a flow reversal system and a distal filter [11]. For two lesions, the Mo.Ma Ultra proximal protection device (Medtronic, Minneapolis, MN, USA) was navigated to occlude the CCA and ECA. Pre-dilatation was performed using a 4.0–5.5 mm Shiden balloon catheter (Kaneka Medix Corporation, Osaka, Japan) with a nominal pressure of 8 atm. A Carotid Wallstent (Stryker, Fremont, California, USA) was deployed. Post-dilatation was performed using a balloon catheter of the same size as those used for pre-dilatation with a nominal pressure of 8 atm. In 3 cases, the stents were overlapped according to the findings of the OCT analysis.

Diffusion weighted (DW)-MRI was performed within 1–2 days after CAS. Carotid ultrasonography or CT angiography was used to evaluate restenosis of the stented lesions. In the case of unstable plaque, dual oral antiplatelets were continued for at least 3 months, whereas in the case of overlapping stents, dual oral antiplatelets were continued for at least 6 months. Subsequently, dual oral antiplatelet regimens were discontinued when in-stent plaque prolapse or restenosis was not detected on ultrasound examination. Single oral antiplatelet administration was continued.

OCT technique

Carotid OCT imaging was performed at pre-procedure, after stent placement, after PD, and after overlapping stent, in cases where it was required. The Dragonfly optical fiber (St Jude Medical, St Paul, Minnesota, USA) used for the investigation of the frequency domain of the OCT system, was encapsulated within a rotating torque wire (0.014 inch compatible) that was used with a rapid exchange 2.6 F catheter compatible with a 6 F guiding catheter to scan a 75 mm artery segment for 2.1 s (pullback speeds up to 36 mm/s). Once the cerebral protection device was deployed in a straight portion of the ICA distal to the stenotic lesion, the calibrated OCT catheter was advanced over the 0.014 inch guide wire of the filter and completely passed over the lesion that needed to be scanned. Pullbacks were started while the CCA and ECA were occluded in cases using balloons mechanically injecting 20 mL of 50% saline diluted contrast medium (Iodixanol 270 mg/mL) to completely replace blood from the artery. Injections were performed through the use of a guiding catheter. Flow arrest within 20 s by occlusion of the CCA and ECA was required to obtain the OCT data. When a guiding catheter without a temporary occlusion balloon was used, pullback was started under the same conditions. After stent deployment, the same OCT maneuvers were repeated.

Assessment of OCT images

OCT data were stored using the available OCT systems (Ilumien Optis Imaging System; St Jude Medical) and analyzed by two experienced OCT readers (HY and MT) using a dedicated software with an automated contour detection algorithm (Off-line Review Software, V.C.0.2; St Jude Medical). Images were considered non-analyzable if any portion of the cross sectional image, other than the guidewire artifact, was out of the screen. The percentage of the stenosis diameter was calculated based on OCT derived North American Symptomatic Carotid Endarterectomy Trial criteria as follows: distal reference lumen diameter—minimal lumen diameter/distal reference lumen diameter $\times 100$.

Definitions of lesion morphology indicating unstable plaque, such as lipid, thin-cap fibroatheroma (TCFA), plaque disruption, ulceration, calcified, thrombus, or macrophage accumulation, were determined based on previous coronary OCT studies [12,13]. TCFA was defined as plaque with lipid content in ≥ 2 quadrants and a fibrous cap with its thinnest part measuring < 65 mm.

Tissue prolapse was defined as the protrusion of tissue between stent struts extending inside a circular arc connecting the adjacent struts. The distance from the arc to the greatest extent of protrusion was used as a quantitative measure [14]. Malapposition was defined when the distance measured from the surface of the blooming (the inner and outer contours of each strut reflection) to the lumen contour was greater than the total thickness of the stent strut plus one-half of the blooming. Regarding carotid stent thickness, a well apposed strut had a protrusion distance rang-

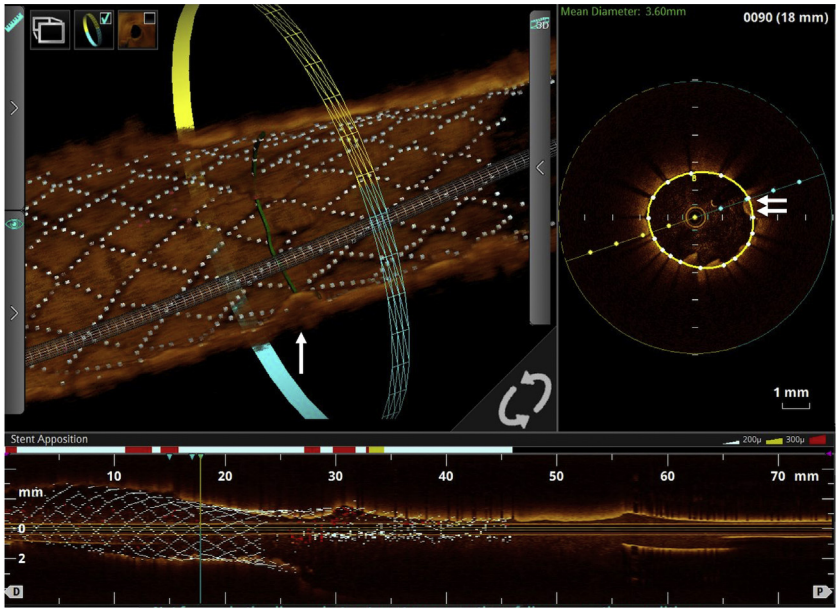

Fig. 1. Three-dimensional (3-D) optical coherence tomography image after stent placement. Numbers of stent cells, numbers of cells with in-stent tissue prolapse and stent malapposition were calculated using proprietary offline review workstation software. In-stent tissue prolapse was detected in 3-D image (arrow) and cross section image (arrows). Yellow circle line indicates stent lumen.

ing from 10 to 200 mm, and a malapposed strut had a protrusion distance > 200 mm [4–6].

Numbers of stent struts, and the number of cells with observed tissue prolapse and malapposition were calculated by 3-dimensional (3-D) navigation mode in the OCT analysis software (Fig. 1). Stent struts were automatically traced by 3-D OCT analysis and supplemented by manual correction.

Pre-procedural minimum lumen diameter and lumen area (LA), and the in-stent lumen diameter (mm) and lumen area (mm^2) were evaluated by 2-dimensional (2-D) cross section images. The corresponding arterial segment in pre-stent images was identified using anatomical landmarks such as carotid bifurcation and analyzed at similar intervals of 1.0 mm. At each interval, the LA and flow area (FA) were measured within the stented segment and tissue prolapse area was defined as LA minus the FA (Fig. 2), i.e.Tissue prolapse area = LA – FA (mm^2).

Statistical analysis

Continuous variables, such as age and creatinine values, are presented as mean (SD). χ^2 analysis and the Fisher exact probability test were performed for categorical variables, such as the rate of tissue prolapse or stent malapposition; $P < 0.05$ was considered significant.

Results

Clinical results

Patient characteristics are shown in Table 1. In symptomatic patients, the mean time from the qualifying event to the OCT study was 50 days (range 20–120 days). Pre-procedural OCT findings, procedural findings, and clinical results are shown in Table 2. Successful revascularization with < 30% residual stenosis in each case was confirmed by angiography. Three lesions with in-stent tissue prolapse ≥ 500 μm were observed after PD, and additional stent was overlapped. No technical or neurological complications occurred during the OCT pullbacks and the CAS procedure. High signal on DW-MRI was detected in 42% patients, and all were asymptomatic. Post-procedural ischemic neurological deficits were not observed during follow-up. Restenosis was not detected in any lesion examined on ultrasound examination.

Table 1
Patient characteristics.

Characteristics	
Age, years, mean ± SD	73 ± 5.8
Men	8
Clinical features	
Hypertension	10
Diabetes	8
Heart disease	9
COPD	3
High carotid position	2
Presenting event	
Minor ischemic stroke	8
Ocular ischemia	1
Asymptomatic	3
Laboratory tests	
Triglyceride (mg/dL)	147 ± 91
LDL cholesterol (mg/dL)	113 ± 19
MRI features	
T1W rSI, mean ± SD	1.83 ± 0.28
T2W rSI, mean ± SD	1.75 ± 0.34
Medication	
Aspirin	12
Clopidogrel	10
Cilostazol	2
Statin	6

COPD: chronic obstructive pulmonary disease; MRI: magnetic resonance imaging; T1W: T1 weighted; rSI: relative signal intensity; T2W: T2 weighted.

OCT results

The OCT evaluation, without artifacts, of continuous 16 to 31 mm-stented segments (mean 20.8 mm), in both after stent placement and PD, including pre-procedural most stenotic lesion, was carried out in this study. OCT findings of lumen diameters and areas are shown in Table 3. Minimum lumen diameters and areas, and mean lumen areas were significantly larger after PD than those after stent placement.

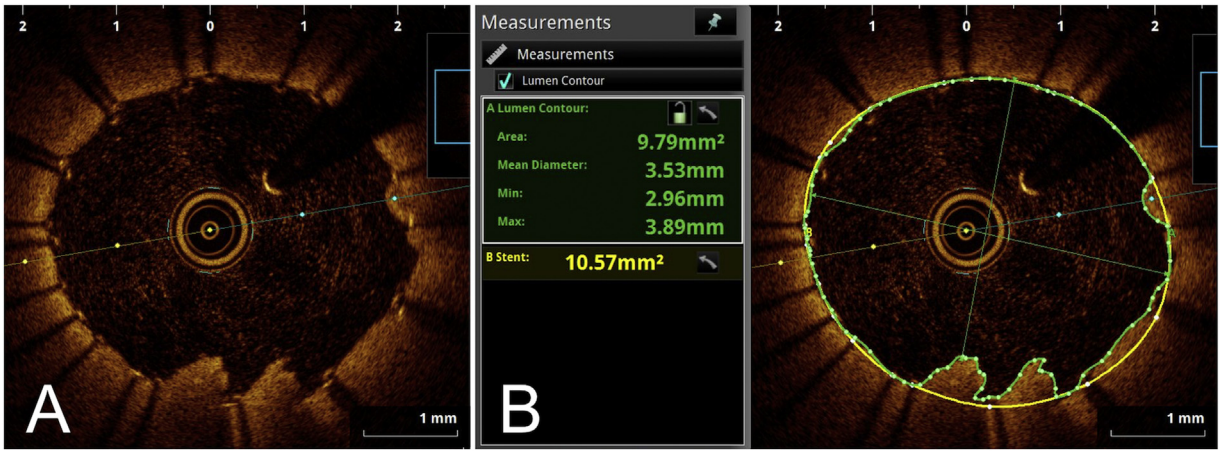

Fig. 2. Assessment method of the tissue prolapse area on optical coherence tomography (OCT) images. The actual measurements of post-stent lumen area and flow areas using the dedicated software in the sample cross section image of the OCT pullback. A. OCT image. B. Stent lumen was traced automatically, supplemented by manual correction. Yellow and green lines indicate stent lumen and flow lumen, respectively, and the lumen areas were calculated automatically. In-stent tissue prolapse volume was calculated as the stent area minus the flow area. In this slice, plaque volume was 0.78 mm^2/slice.

Table 2
OCT results and clinical course.

OCT results	
Plaque morphology, *n*	
Lipid	12
Calcification	2
Ulceration	9
TCFA	12
Disruption	9
Thrombus	1
Neovascularization	4
Measured length, mm	20.8 ± 6.3
Stent cells, n	271 ± 68
OCT-NASCET, %	71 ± 8.7
Area of most stenotic lesions, mm^2	2.6 ± 1.6
Diameter of most stenotic lesions, mm^2	1.5 ± 0.6
Pre-and post-dilatation balloon size, mm	4.8 ± 0.3
Size of closed-cell stent, *n*	
6 mm	1
8 mm	5
10 mm	6
Overlapping stent, *n*	3
Clinical course	
Neurological deficits, *n*	0
DW-MRI high-signal spots, *n*	5
Duration of DAPT, months	3.6 ± 1.9
Follow up, months	10.6 ± 2.9
Restenosis, *n*	0
Delayed ischemic stroke, *n*	0

OCT: optical coherence tomography; TCFA: thin-cap fibroatheroma; NASCET: North American Symptomatic Carotid Endarterectomy Trial; DW-MR: Diffusion weighted-magnetic resonance imaging; DAPT: dual antiplatelet therapy.

OCT findings of the in-stent tissue prolapse volume, and the stent cell numbers of tissue prolapse and malapposition are shown in Table 3. Compared to after stent placement, the mean in-stent tissue prolapse volume, stent cells with any tissue prolapse were significantly increased after PD; however, stent cells with ≥ 500-μm tissue prolapse and stent malapposition were significantly reduced. Representative lesion which stent cells with ≥ 500-μm tissue prolapse were significantly reduced after PD was presented in Fig. 3. The change of the rates in which stent cells with ≥ 500-μm tissue prolapse, any tissue prolapse, and malapposition were shown in Fig. 4.

OCT evaluation after overlapping stents in 3 lesions demonstrated that in-stent tissue prolapse volumes were significantly decreased by the use of the overlapping stent (from 0.23 ± 0.05 to 0.13 ± 0.05 mm^2/slice, $P < 0.05$).

Table 3
OCT findings after post stent placement and after post-dilatation.

	Post-stent placement	Post-dilatation	*P*-value
Minimum lumen			
Diameter, mm	3.2 ± 0.7	3.6 ± 0.6	< 0.001
Area, mm^2	10.2 ± 3.7	12.0 ± 3.3	< 0.001
Mean lumen area, mm^2	15.0 ± 3.9	16.6 ± 3.78	< 0.001
In-stent tissue prolapse volume, mm^2/slice	0.18 ± 0.10	0.22 ± 0.07	< 0.01
Stent cells			
Any tissue prolapse, %	12.7 ± 8.2	21.0 ± 11.8	< 0.001
≥500-μm tissue prolapse, %	1.6 ± 1.1	0.7 ± 0.8	< 0.01
Malapposition, %	17.4 ± 7.2	14.0 ± 6.3	< 0.01

OCT, optical coherence tomography

In 42% (5/12) of the lesions, post-procedural DW-MRI high-signal spots (DW positive group) were detected. There were no significant differences in in-stent tissue prolapse volume after PD between the DW-positive and negative groups (0.23 ± 0.08 vs 0.21 ± 0.07 mm^2/slice, $P = 0.30$). There were also no significant differences in the proportion of stent cells with ≥ 500-μm tissue prolapse after PD between the DW-positive and negative groups (0.77 ± 0.60 vs. 0.60 ± 1.03%, $P = 0.38$).

Discussion

In this study, it was observed that stent struts with tissue prolapse and in-stent tissue prolapse volume were significantly higher after PD for unstable plaque using CC stent; however, tissue prolapse ≥ 500-μm was significantly less.

Tissue prolapse between stent struts could cause post-procedural embolism after CAS [6,15,16]. Delayed embolism after CAS was probably caused by the fractured plaque deposits through the stent struts, migration of in-stent tissue prolapse, and stent thrombosis. This is especially true for unstable plaque including lipid-rich plaque and intra-plaque hemorrhage, which could prolapse through the stent struts due to its softness and its liquid components [2]. Pre- and intra-procedural predictors of tissue prolapse were unstable plaque and the use of an open-cell design stent [5,15]. CC stent had used expectantly to prevent plaque prolapse for unstable carotid lesions; however, even CC stents could not overcome the problem of tissue prolapse for unstable carotid plaques [6]. The recently developed technology of dual layer stent has significantly decreased tissue prolapse compared to the conventional

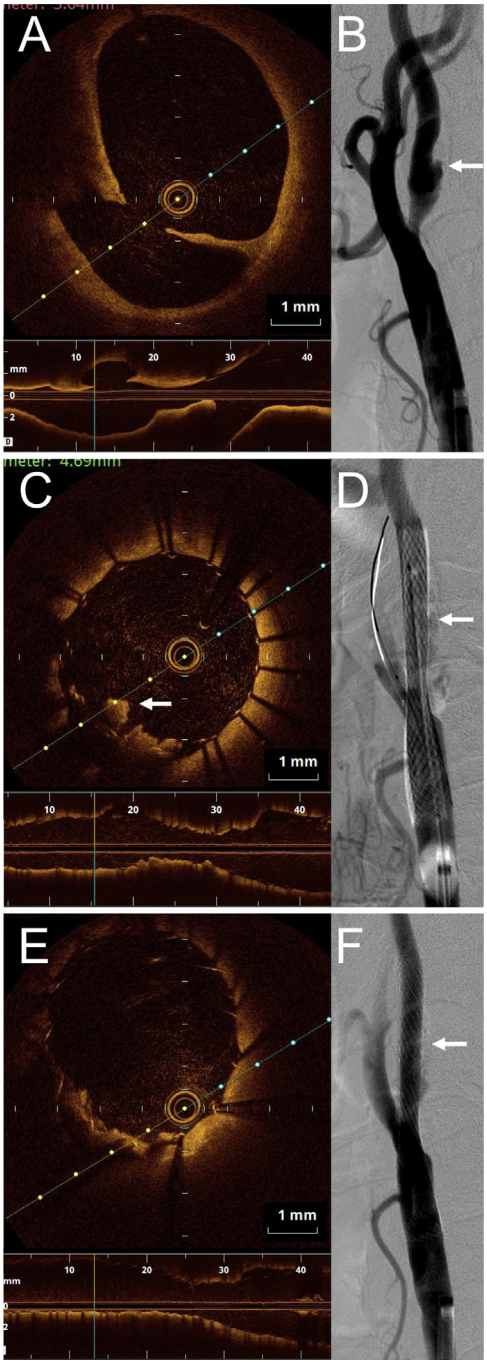

Fig. 3. Representative case showing that in-stent large tissue prolapse (≥ 500 μm) is decreased after post-dilatation. A. Pre-procedural optical coherence tomography (OCT) indicated ulceration and lipid-rich plaque. B. Angiogram of pre-procedural carotid stenosis. C. After stent placement, large tissue prolapse (arrow) between the struts were observed by OCT. D. Angiogram after stent placement. E. After post-dilatation, in-stent large tissue prolapse decreased, whereas in-stent small (< 500 μm) tissue prolapse increased by OCT analysis. F. Post-procedural angiogram revealed good revascularization. Arrows in B, D, and F indicate the corresponding location of OCT analysis.

stent; nevertheless, plaque prolapse was observed in the OCT analysis [17].

PD contributes stent expansion; however, it may cause debris formation. The CAS technique includes initial lesion crossing the stenotic lesion using an EPD system or a guidewire, subsequent balloon pre-dilatation to cross the stent, followed by stent placement to cover the plaque, and finally PD to achieve stent expansion. PD crushes the friable plaque against the metal stent, and can cause emboli. Vos et al. reported using transcranial Doppler (TCD) studies that the generation of emboli with the highest potential for embolization occurs during PD [8]. Ackerstaff et al. demonstrated in a study of 550 patients that multiple microemboli (> 5 showers) at PD were independently associated with cerebral deficits [18]. To prevent intra-procedural embolic complications, CAS without PD had been considered. Ogata et al. studied 169 carotid lesions and reported that CAS without PD had low rates (1.1%) of ischemic stroke within 30-days. They used distal balloons or filter protection as EPD, large angioplasty balloons (4.0–5.5 mm), and CC stents (98.9% of the lesions) without PD. However, residual stenosis > 30% was observed in 16% patients immediately after CAS and delayed ischemic embolization and restenosis were observed in 7.4% and 11.1% patients, respectively; these were significantly higher rates compared to that of residual stenosis > 30% immediately after CAS [9]. Thus, CAS without PD was safe method in the short term, however, the problems of insufficient stent dilatation, delayed ischemic embolization, and long-term restenosis were not solved.

In this study, any tissue prolapse was increased, however, tissue prolapse ≥ 500-μm was decreased by PD. These results suggested that some parts of the in-stent tissue prolapse was fractured as debris by PD. Thus, PD may decrease delayed embolic complications and restenosis due to decreased in-stent tissue prolapse and stent expansion. Based on the results of this study, we believe that PD should be performed to increase in-stent lumen diameter and decrease large tissue prolapse between the stent struts even for an unstable plaque lesion in cases in which sufficient EPD (such as proximal protection or a combined protection of proximal protection and distal filter), which can retrieve much debris, is achieved. In cases with ≥ 500-μm tissue prolapse after PD, which causes delayed migration, additional PD should be primarily performed to reduce tissue prolapse. In case a large amount of tissue prolapse remains, an additional closed-cell (CC) stent may be overlapped with in the initial stent [6]. In contrast, PD might not be avoided for unstable plaque in case sufficient EPD is not achieved, such as in cases that involve only the use of a distal filter, which cannot retrieve much debris.

This study had some limitations. This was a single center study with a limited number of patients. There was no control group in this study, and the selected lesions predominantly comprised unstable plaques, non-elongated lesions, and lesions treated by same-size balloon catheters pre- and post-dilatation. There were also some limitations with regard to OCT for carotid lesions. OCT evaluation was difficult in elongated lesions because the OCT system could not reach the elongated ICA distal to the culprit lesion. OCT studies required a blood-free environment; therefore, mechanical injection of half of the concentration of the contrast medium was increased during the procedure. The penetration depth for OCT was 5–6 mm; therefore, the CCA lesions were prone to out of screen artifacts. The details of the carotid lesion by OCT evaluation in the pre-procedural and the post-stent evaluation could be a little mismatched as the carotid artery was stretched by the placement of the CC stent. In OCT analysis, small plaque prolapse may be confused with a small thrombus: red thrombus is detected as highly backscattering with a high attenuation, and white thrombus is detected as less backscattering, homogeneous, and with low attenuation [13]. In this study, almost all of tissue prolapse from the stent struts was considered to be plaque, however, it might be difficult to differentiate between small plaque prolapse and small thrombus.

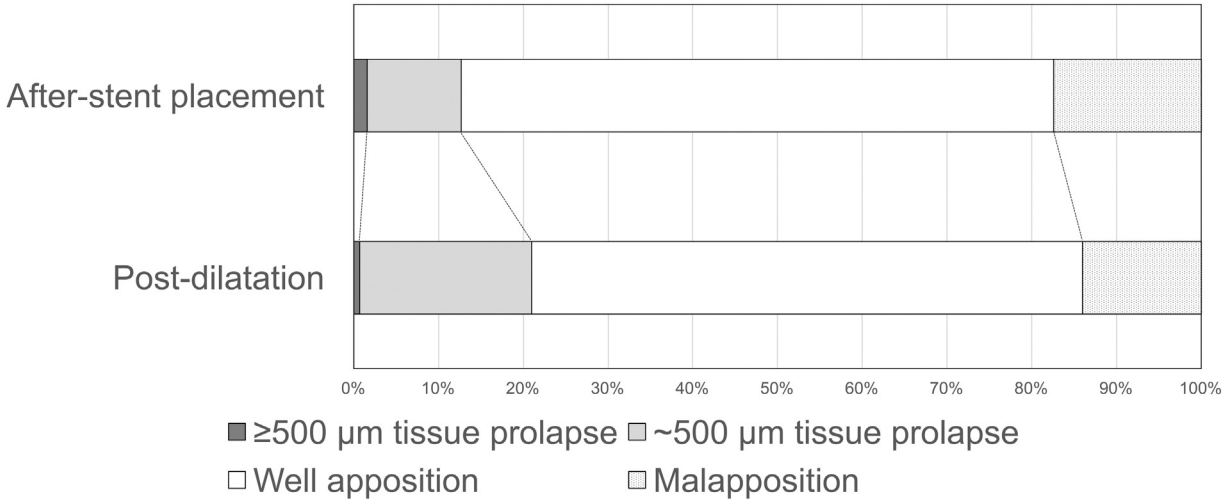

Fig. 4. The number of stent cells observed tissue prolapse and malapposition after stent placement and after post-dilatation.

Conclusion

After PD for unstable plaque using closed-cell design stent, we observed that the stent was expanded and any tissue prolapse was increased; however, tissue prolapse ≥ 500-μm was decreased. PD may decrease delayed ischemic events by expanding the stent and decreasing large in-stent tissue prolapse by crushing the in-stent tissue prolapse into debris. In CAS for unstable plaque with PD, sufficient EPD was needed to prevent intra-procedural emboli.

Funding

This research did not receive any specific grant from funding agencies in the public, commercial, or not-for-profit sectors.

Contributors

KH was the main operator of the endovascular treatment, designed the research, and drafted the manuscript. MK, YS and ST were the main assistants in the endovascular treatment and reviewed the manuscript.

Disclosure of interest

The authors declare that they have no competing interest.

Acknowledgement

The authors thank Yutarou Hirayama and Toshiya Morinaga (medical engineers, Fukuoka Wajiro Hospital) for help with the analysis of the OCT frames.

References

[1] Brott TG, Hobson II RW, Howard G, et al. Stenting versus endarterectomy for treatment of carotid-artery stenosis. N Engl J Med 2010;363:11–23.
[2] Yamada K, Yoshimura S, Kawasaki M, et al. Embolic complications after carotid artery stenting or carotid endarterectomy are associated with tissue characteristics of carotid plaques evaluated by magnetic resonance imaging. Atherosclerosis 2011;215:399–404.
[3] Müller-Hülsbeck S, Schäfer PJ, Charalambous N, et al. Comparison of carotid stents: an in-vitro experiment focusing on stent design. J Endovasc Ther 2009;16:168–77.
[4] de Donato G, Setacci F, Sirignano P, et al. Optical coherence tomography after carotid stenting: rate of stent malapposition, plaque prolapse and fibrous cap rupture according to stent design. Eur J Vasc Endovasc Surg 2013;45:579–87.
[5] Liu R, Jiang Y, Xiong Y, et al. An optical coherence tomography assessment of stent strut apposition based on the presence of lipid-rich plaque in the carotid artery. J Endovasc Ther 2015;22:942–9.
[6] Harada K, Oshikata S, Kajihara M. Optical coherence tomography evaluation of tissue prolapse after carotid artery stenting using closed cell design stents for unstable plaque. J Neurointerv Surg 2018;10:229–34.
[7] Montorsi P, Caputi L, Galli S, et al. Microembolization during carotid artery stenting in patients with high-risk, lipid-rich plaque. A randomized trial of proximal versus distal cerebral protection. J Am Coll Cardiol 2011;58:1656–63.
[8] Vos JA, van den Berg JC, Ernst SM, et al. Carotid angioplasty and stent placement: comparison of transcranial Doppler US date and clinical outcome with and without filtering cerebral protection devices in 509 patients. Radiology 2005;234:493–9.
[9] Ogata A, Sonobe M, Kato N, Yamazaki T, Kasuya H, Ikeda G, Miki S, Matsushima T. Carotid artery stenting without post-stenting balloon dilatation. J Neurointerv Surg 2014;6:517–20.
[10] Yoshimura S, Kawasaki M, Yamada K, et al. Visualization of internal carotid artery atherosclerotic plaques in symptomatic and asymptomatic patients: a comparison of optical coherence tomography and intravascular ultrasound. AJNR Am J Neuroradiol 2012;33:308–13.
[11] Harada K, Kakumoto K, Morioka J, et al. Combination of flow reversal and distal filter for cerebral protection during carotid artery stenting. Ann Vasc Surg 2014;28:651–8.
[12] Bezerra HG, Costa MA, Guagliumi G, et al. Intracoronary optical coherence tomography: a comprehensive review clinical and research applications. JACC Cardiovasc Interv 2009;2:1035–46.
[13] Tearney GJ, Regar E, Akasaka T, et al. Consensus standards for acquisition, measurement, and reporting of intravascular optical coherence tomography studies: a report from the International Working Group for Intravascular Optical Coherence Tomography Standardization and Validation. J Am Coll Cardiol 2012;59:1058–72.
[14] Bouma BE, Tearney GJ, Yabushita H, et al. Evaluation of intracoronary stenting by intravascular optical coherence tomography. Heart 2003;89:317–20.
[15] Kotsugi M, Takayama K, Myouchin K, et al. Carotid artery stenting: investigation of plaque protrusion incidence and prognosis. JACC Cardiovasc Interv 2017;24:824–31.
[16] Beppu M, Mineharu Y, Imamura H, et al. Postoperative in-stent protrusion is an important predictor of perioperative ischemic complications after carotid artery stenting. J Neuroradiol 2018, http://dx.doi.org/10.1016/j.neurad.2018.02.009.
[17] Yamada K, Yoshimura S, Miura M, et al. Potential of new-generation double-layer micromesh stent for carotid artery stenting in patients with unstable plaque: a preliminary result using OFDI Analysis. World Neurosurg 2017;105:321–6.
[18] Ackerstaff RG, Suttorp MJ, van den Berg JC. Prediction of early cerebral outcome by transcranial Doppler monitoring in carotid bifurcation angioplasty and stenting. J Vasc Surg 2005;41:618–24.

Glossary

Thin-cap fibroatheroma (TCFA): Plaque with lipid content in ≥2 quadrants and a fibrous cap with its thinnest part measuring <65 mm
Tissue prolapse: The protrusion of tissue between stent struts extending inside a circular arc connecting the adjacent struts
Malapposition: The distance measured from the surface of the blooming (the inner and outer contours of each strut reflection) to the lumen contour was greater than the total thickness of the stent strut plus one-half of the blooming